NASA Technical Memorandum 83398

NASA Low-Speed Centrifugal Compressor For Fundamental Research

Jerry R. Wood, Paul W. Adam, and Alvin E. Buggele
Lewis Research Center
Cleveland, Ohio

Prepared for the
Nineteenth Joint Propulsion Conference and Technical Display
cosponsored by the AIAA, SAE, and ASME
Seattle, Washington, June 27-29, 1983

NASA

NASA LOW-SPEED CENTRIFUGAL COMPRESSOR FOR FUNDAMENTAL RESEARCH

Jerry R. Wood, Paul W. Adam, and Alvin E. Buggele

National Aeronautics and Space Administration
Lewis Research Center
Cleveland, Ohio 44135

Abstract

A new centrifugal compressor facility being built by the NASA Lewis Research Center is described; its purpose is to obtain "benchmark" experimental data for internal flow code verification and modeling. The facility will be heavily instrumented with standard pressure and temperature probes and have provisions for flow visualization and laser Doppler velocimetry. The facility will accommodate rotational speeds to 2400 rpm and will be rated at pressures to 1.25 atm. The initial compressor stage for testing is geometrically and dynamically representative of modern high-performance stages with the exception of Mach number levels. Design exit tip speed for the initial stage is 500 ft/sec with a pressure ratio of 1.17. The rotor exit backsweep is 55° from radial. The facility is expected to be operational in the first half of 1985.

Introduction

In the past decade both industry and government have placed increased emphasis on improving the performance of small, gas turbine engines. In the last few years NASA and the Army have embarked on a major research program intended to provide the necessary information and tools to advance both component and system technology. Three analytical studies were conducted under contract to determine appropriate configurations for small, high-performance gas turbine engines in the 1990 time frame. The results were based on initial cost, performance, reliability, etc., and indicated that an axial/centrifugal compressor staging arrangement would be a strong candidate for engines operating with core mass flows of 10 lb/sec or less. Much progress has been made in improving compressor performance by using empirical design procedures. These procedures require an extensive data base. However, further gains in performance for both axial and centrifugal compressors are expected to be obtained by using advanced computational codes in design and analysis. To provide a more thorough understanding of the flow in the complex geometric channels of the centrifugal compressor, NASA has embarked on several experimental programs that are focused on obtaining "benchmark" experimental data in both transonic and subsonic flow regimes. One of these efforts is to design and fabricate a large, low-speed centrifugal compressor that can be used to verify three-dimensional viscous codes and to provide data with which to develop more sophisticated models of the various physical phenomena occurring in a centrifugal compressor.

The centrifugal compressor flow passage represents an amalgam of complex phenomena depicted in figure 1. This figure represents what one might imagine occurs as the flow progresses from the inlet to the outlet of the machine. These effects include shocks, secondary flows generated by inlet vorticity, secondary flows generated when boundary layers are subjected to transverse forces, tip clearance flows, and turbulence suppression and enhancement due to strong normal pressure gradients occurring across the boundary layer in the radial portion of the compressor. The diffuser vanes are subjected to an unsteady, three-dimensional flow exiting from the impeller. The impeller, in turn, is subjected to an unsteady backpressure by the diffuser vanes. Past experiments to measure these phenomena and thereby to achieve some useful data whereby models of the flow physics could be generated have ranged from simple channel experiments[1-4] to actual compressors.[5-8] Each has produced information that provides us with better insight into the physical processes occurring in a rotating channel. Considerable effort has been expended in obtaining quite detailed measurements of the flows in large axial compressors in an attempt to develop models that reflect the flow processes in actual blade rows.[9-12] This paper describes a facility being constructed by NASA to obtain comparable data in a large centrifugal compressor.

Facility

Figure 2 shows the major elements of the facility. Air will be drawn in from a filtered vent in the roof and into the plenum through a bank of flow straighteners. The flow will then pass through a series of screens to further reduce the turbulence level. The area contraction into the specially designed bellmouth will be 10:1. This combination should produce turbulence levels at the rotor inlet of less than 1 percent. The bellmouth, the inlet transition piece, and the shroud flow path will be finished machined together to minimize any boundary layer disturbance due to a step in the flow path. The flow will then enter the compressor and exit through a throttle valve at the entrance to the collector. The valve will consist of two rings with 4-in.-diameter holes drilled in each ring so that circumferential translation of one ring will reduce the available flow area. Close coupling the throttle valve in this manner will minimize the volume that influences surge of the stage and aid in establishing a uniform flow field around the periphery of the machine. The drive motor for the facility will be a 1500-hp electric motor that will drive through a gear reducer to obtain a 33 percent reduction in drive motor speed to a maximum output speed of 2400 rpm. The facility will be designed for a nominal airflow of 66 lb/sec and a rated maximum pressure of 1.25 atm. The facility piping will be sized to allow operation using atmospheric exhaust over most of the pressure ratio map. An altitude exhaust capability of 26 in. of vacuum will be available to obtain the high-flow portion of a speed line. The facility will be able to handle rotors up to 6 ft in diameter and will be nominally designed for rotors operating at exit tip speeds to 500 ft/sec. Flow visualization capability will be provided via a system of feed-throughs so that smoke can be carried into the rotating reference frame of the rotor. The rotor will be mounted horizontally as shown, and because of its overhung

bearing configuration the rotor will droop by approximately 0.019 in. at the leading edge. To prevent a large variation in clearance around the periphery of the wheel, provisions have been made to adjust the shroud so that a uniform clearance can be obtained. Clearance around the wheel will be measured dynamically by using optical clearance probes at the inlet, near midchord, and near the exit.

Instrumentation

Instrumentation for the facility will include a torquemeter for measuring overall work input and standard aerodynamic survey probes (total pressure and temperature and flow angle) at the rotor inlet, the rotor exit, and the diffuser exit. A block diagram of the research instrumentation is shown in figure 3. All pressure measurements will be controlled through a host computer that will update the calibration of each pressure transducer periodically throughout the test. Another dedicated computer will control the position of all aerodynamic survey probes so that surveys can be done automatically during testing. When desired, these computers will transmit appropriate data to the Lewis Central Data Acquisition System (LCDAS). All other data will be transferred directly to the LCDAS. Dynamic instrumentation measurements will be stored on magnetic tape for further processing. The rotor itself will be heavily instrumented as shown in figure 4. Approximately 170 static pressure measurements will be taken on the rotor at 10 different planes in the throughflow direction with another 18 on the rotating spinner. Three planes will be instrumented with 75 total pressure tubes and 9 total temperature probes. These measurements will be used in conjunction with the laser measurements to determine the local thermodynamic state at these planes. Originally, we had planned to use actuator systems on the rotor; however, the centrifugal loading of nearly 3000 g's at the exit tip speed of 500 ft/sec indicated that a special development program would be required to obtain a suitable system. The total pressure probes mounted on the rotor will cover the passage at 5, 20, 50, 80, and 95 percent of span and pitch. Total temperature probes will be located at 20, 50, and 80 percent of span and pitch. Pressure- and temperature-sensing elements will be set at least three rake diameters upstream to minimize stem effects, and only one rake will be located in a passage to minimize flow blockage effects due to the probes. Qualification tests are being conducted on the rake design so that its cross-sectional area can be minimized while maintaining a structurally sound probe. Each pressure rake will have five elements in the spanwise direction, and each thermocouple rake will have three elements in the spanwise direction. At all three survey planes the pressure at the 5- and 95-percent-of-pitch locations will be sensed by using 0.060-in-o.d. stainless steel tubing mounted on the blade at each percent-of-span location. These blade-mounted probes will also be used at the 20- and 80-percent-of-pitch locations at station 1 because the pitchwise spacing will be too small to accommodate the rakes. Both types of quick-disconnect rakes will be removable from the rotor through the openings for the optical windows and can be replaced with plugs to maintain the hub contour. None of the rakes will be located in the passage containing the static taps.

Since the rotor will operate at relatively low speeds, the pressure differentials that will tend to drive the secondary flows will be quite small. The geometry of the initial design has been analyzed with a three-dimensional Euler code. The resultant pressure distributions indicate that pressure differences from blade to blade and from hub to shroud will vary from approximately 0.0145 psi to 0.70 psi. Pressure taps will be located at 5, 20, 50, 80, 95, and 99 percent of span along the blade and at 5, 20, 50, 80, and 95 percent of pitch across the hub. Thus in some areas of the channel we will need to measure pressure differences as small as 0.0014 psi. To achieve this level of resolution of the pressure gradients (i.e., we primarily desire the values of the pressures relative to one another), a pressure-measuring device that can measure pressures accurately to within 0.001 psi will be used. The pressure modules to be used will consist of 48 silicon pressure sensors housed in a rectangular module 1.2 in. by 2.7 in. by 1.5 in. that will be mounted on the centerline of the rig so that no portion of the module will be more than 1.35 in. from the centerline. The diaphragms will be oriented perpendicular to the centerline. Six of these modules will be installed in the spinner of the rotor, where the thermal environment should be stable. During operation each pressure transducer will be dynamically calibrated by transfering three known calibration pressures to the modules through a rotating feedthrough located on the shaft behind the compressor housing. These calibration pressures and calibration pressures for stationary pressure measurements will be monitored by using a digital pressure transducer with an accuracy of 0.01 percent of full scale. Reference pressures for the differential transducers will be set by using a deadweight. The modules will be set to check one another during operation by reading the same pressure tap with all six modules in order to reduce relative errors. Errors associated with reading the pressures while the modules are under the influence of rotation will be reduced by monitoring a total pressure tube on the front of the spinner. This tube should sense the same total pressure as that measured in the plenum by the stationary pressure-measuring system. Appropriate corrections to the indicated rotating pressures can be made during data processing or on line by using the host computer for the pressure-sensing system.

Reading pressures in a rotating frame will produce some problems that are normally not encountered. The pressure taps will be arranged along the flow path, and stainless steel tubes will be routed down the back of the rotor to the six pressure-measuring modules located in the rotor hub. Therefore the pressure sensed at the pressure transducers will not be the same as that we wish to measure because of the centrifugal head of the air in the tubes produced by rotation. This effect will be substantial even in a low-speed facility such as this and must be accounted for. Techniques have been developed at Lewis to account for this pressure rise during data reduction. To obtain pressure measurements with sufficient accuracy, it is necessary to determine the temperature distribution of the air inside the tubing. This will be accomplished by means of thermocouples set along the tube path. The rotor back face will contain 16 radial ribs to minimize deflections at design speed. To prevent pumping of the flow

on the back face due to the ribs, they will be covered by a flat plate. This will trap a quantity of air approximately 3 in. thick over the entire back face and thus essentially bathe the pressure tubes in air undergoing solid-body rotation. Since the air will be undergoing solid-body rotation, we will be able to calculate its temperature distribution and compare it with the thermocouple readings for consistency.

Optical windows for use with flow visualization and laser velocimetry will be provided at the inlet, the knee region, and the exit region. The window at the rotor exit will be sized to view inside the rotor when the diffuser is in place. This will allow measurement of the unsteady flow field imposed on the rotating rotor by the diffuser vanes. The laser Doppler velocimeter (LDV) system to be used will consist of an argon-ion laser coupled with appropriate optics to yield a probe volume measuring approximately 0.025 in. long by 0.0033 in. diameter. The LDV system will be moved by means of translating tables (slides) in the x, y, and z directions and by a rotary table as shown in figure 4. The table drives will be remotely positioned by a dedicated minicomputer to preprogrammed measurement points, and data will be recorded automatically. Data will be inspected on line to determine acceptability and processed later for presentation graphically. Locations of the LDV windows are also shown in figure 4. The inlet and knee region windows will be 4 in. wide and approximately 15 in. and 6 in. long, respectively. They will cover the flow path from 9.5 in. upstream of the rotor to 3.5 in. from the rotor exit with a blind area for frames from 5 to 8 in. from the rotor inlet. The diffuser window will start 3 in. upstream of the rotor exit and extend 12 in. radially downstream. It will be approximately 14 in. wide and cover the rotor exit, the vaneless space, and the throat region of the diffuser.

Initial Stage Design

The initial compressor for this facility was designed with a twofold purpose: first, that the geometry should be representative of that typically found in high-performance centrifugal machines; and second, that optical access to the blade boundary layers should be maximized by minimizing "shadow" regions caused by blade lean. The resulting stage parameters are tabulated in table I. The stage develops a total pressure ratio of 1.17 with an estimated efficiency of 0.90 at the design flow of 66 lb/sec. The design rotational speed is 1920 rpm with an exit tip speed of 500 ft/sec. Inlet impeller tip relative Mach number is 0.31, and exit tip absolute Mach number is 0.29. The impeller blade backsweep at the exit is 55°, and the inlet hub-tip radius ratio is 0.5. The compressor Reynolds number based on impeller exit diameter and tip speed is 1.6×10^7, which is comparable to that of current high performance machines. The initial configuration will have a wedge diffuser that will be removed for the initial tests so that the impeller exit flow is not influenced by the periodic disturbance created by the diffuser vanes.

The rotor was designed by using a preliminary design code for centrifugal compressors recently developed at Lewis. Detailed geometry was generated by using a Lewis-developed code for arbitrary turbomachinery blade shapes that uses as its analysis subroutine the code described in reference 13. The meridional hub and shroud contours for the rotor are shown in figure 5(a) and are composed of superellipses that have smooth, continuous curvatures. The diffuser has simple wedge vanes inclined to the radius at 76°. The area ratio of 2.9 was selected to give good pressure recovery (based on the experimental maps of ref. 14) at the calculated inlet blockages and Mach number. The blade angle distributions in figure 5(b) were chosen to achieve smooth velocity distributions while maintaining minimum blade lean. The normal thicknesses (fig. 5(c)) for the blading yielded adequate structural strength, and the blade blockages are representative of those found on small machines. The thicknesses shown in figure 5(c) reflect the addition to the leading edge of an ellipse that is continuous in the first derivative at its junction with the blade. The resulting leading edge will produce a smooth transition of the flow onto the blade.

Figure 6 gives the vector diagrams for the rotor and the relative Mach number distribution over the rotor blading. The diagrams are typical of those calculated for high-performance centrifugal compressors with the obvious exception of the Mach numbers, which are considerably lower. The Mach numbers in the rotor were calculated by using a three-dimensional Euler code as described in reference 15 and demonstrate that the goal of obtaining smooth velocity distributions was attained. Two-dimensional boundary layer calculations indicate boundary layer thicknesses of approximately 1 in. near the rotor exit.

Table II is a comparison of this stage with some typical centrifugal compressor stages. It is intended to demonstrate that information obtained on this machine will be useful for verifying advanced viscous codes and for modeling the phenomena occurring in centrifugal compressor stages. Reynolds numbers, specific speed, rotor backsweep, diffuser area ratio, and channel divergence have been chosen to reflect geometry and nondimensional parameters comparable to modern machines.

Concluding Remarks

A new facility being developed by the NASA to obtain detailed internal flow measurements inside a large, low-speed centrifugal compressor has been described. Its primary use will be to provide experimental data for verifying advanced computer codes and for developing detailed models to describe the flow occurring in a centrifugal compressor. Measurements will be made by using both laser Doppler velocimetry and standard aerodynamic probes. Flow visualization will be used to enhance understanding of the qualitative aspects of the flow. The facility is expected to be operational by mid-1985.

Appendix - Symbols

b	blade height, in.
C_p	pressure recovery coefficient, $(p_i - p_{i-1})/(p'_{i-1} - p_{i-1})$
D	diameter, ft
H	ideal head rise, ft
M	Mach number

N rotational speed, rpm
P pressure, lbf/ft^2
Q inlet flow rate, ft^3/sec
U rotor speed, ft/sec
V absolute velocity, ft/sec
W relative velocity, ft/sec
ν kinematic viscosity, ft^2/sec

Subscript:

i station number
rel relative to rotor
0 plenum
1 rotor inlet
2 rotor exit

Superscript:

' total condition

References

1. Moon, I. M., "Effect of Coriolis Force on the Turbulent Boundary Layer in Rotating Fluid Machines," Massachusetts Institute of Technology, Gas Turbine Laboratory Report No. 74, June 1964.
2. Moore, J., "The Development of Turbulent Boundary Layers in Centrifugal Machines," Massachusetts Institute of Technology, Gas Turbine Laboratory Report No. 99, June 1969.
3. Johnston, J. P., Halleen, R. M., and Lezuis, D. K., "Effects of Spanwise Rotation on the Structure of Two-Dimensional Fully Developed Turbulent Channel Flow," Journal of Fluid Mechanics, Vol. 56, Pt. 3, 1972, pp. 533-557.
4. Rothe, P. H. and Johnston, J. P., "The Effects of System Rotation on Separation, Reattachment and Performance in Two-Dimensional Diffusers," Stanford University Report PD-17, May 1975.
5. Fowler, H. S., "The Distribution and Stability of Flow in a Rotating Channel," Journal of Engineering for Power, Vol. 90, No. 2, July 1968, pp. 229-236.
6. Johnson, M. W. and Moore, J., "The Influence of Flow Rate on the Wake in a Centrifugal Impeller," ASME Paper 82-GT-45, Apr. 1982.
7. Eckardt, D., "Detailed Flow Investigations Within a High-Speed Centrifugal Compressor Impeller," ASME Paper 76-FE-13, Mar. 1976.
8. Adler, D., and Levy, ..., "A Laser-Doppler Investigation of the Flow Inside a Backswept, Closed, Centrifugal Impeller," Journal of Mechanical Engineering Science, Vol. 21, No. 1, Feb. 1979, pp. 1-6.
9. Wagner, J. H., Dring, R. P., and Joslyn, H. D., "Axial Compressor Middle Stage Secondary Flow Study," NASA Contract NAS3-23157 (To be published as NASA Contractor Report), 1983.
10. Bettner, J. L. and Elrod, C., "The Influence of Tip Clearance, Stage Loading, and Wall Roughness on Compressor Casing Boundary Layer Development," ASME Paper 82-GT-153, Apr. 1982.
11. Wisler, D. C., "Core Compressor Exit Stage Study," General Electric Co., Cincinnati, OH, GE-R81AEG288, Dec. 1981. (NASA CR-165553).
12. Lakshminarayana, B., "An Axial Flow Research Compressor Facility Designed for Flow Measurement in Rotor Passages," ASME Journal of Fluids Engineering, Vol. 102, No. 4, Dec. 1980, pp. 402-411.
13. Katsanis, T. and McNally, William D., "Revised Fortran Program for Calculating Velocities and Streamlines on the Hub-Shroud Midchannel Stream Surface of an Axial-, Radial-, or Mixed-Flow Turbomachine or Annular Duct: Part I - User's Manual," NASA TN D-8430, Mar. 1977.
14. Runstadler, P. W., Jr., "Pressure Recovery Performance of Straight-Channel, Single-Plane Divergence Diffusers at High Mach Numbers," USAAVLABS Technical Report 69-56, Oct. 1969.
15. Denton, J. D., "An Improved Time Marching Method for Turbomachinery Flow Calculation," ASME Paper 82-GT-239, Apr. 1982.

TABLE I. - DESIGN PARAMETERS FOR LOW-SPEED CENTRIFUGAL COMPRESSOR

Stage:	
Flow rate, lb/sec	66
Total pressure ratio	1.166
Estimated efficiency	0.90
Rotor:	
Total pressure ratio	1.173
Estimated efficiency	0.934
Inlet hub-tip ratio	0.5
Inlet span, in.	8.678
Inlet tip radius, in.	16.905
Exit radius, in.	3 .00
Exit blade height, in.	5.4096
Clearance, in.	0.225
Number of blades	20
Reynolds number, U_2D_2/ν_0	16×10^6
Inlet tip relative Mach number	0.31
Exit absolute Mach number	0.29
Diffuser:	
Ratio of vane inlet radius to rotor exit radius	1.08
Number of vanes	23
Leading-edge circle radius, in.	0.161
Pressure surface angle, deg	72
Suction surface angle, deg	80
Channel divergence, deg	7.65
Area ratio	2.9
Throat aerodynamic blockage, percent	2
Throat Mach number	0.263
Exit Mach number	0.08
Inlet Reynolds number, b_2V_2/ν_2	10^6
Pressure recovery coefficient, C_p:	
Rotor exit to throat	0.20
Throat to trailing edge	0.72

TABLE II. - COMPARISON OF LOW-SPEED CENTRIFUGAL COMPRESSOR TO TYPICAL STAGES

Parameter	Low speed	Stage 1	Stage 2	Stage 3	Stage 4
Stage:					
Flow rate, lb/sec	66	2.3	10	10	25
Rotational speed, rpm	1920	68 384	21 789	36 366	23 000
Pressure ratio	1.17	6.0	4.0	8.0	8.0
Reynolds number, U_2D_2/ν_0	16×10^6	6.3×10^6	15×10^6	21×10^6	33×10^6
Specific speed, $N\sqrt{Q}/(H)^{3/4}$	104	89	76	93	93
Rotor:					
Rotor exit tip speed, ft/sec	500	1891	1655	2007	2007
Rotor inlet tip relative Mach number	0.31	1.15	0.88	1.39	1.39
Blade angle at inlet tip, deg	56.3	61.4	55.8	61.4	61.4
Blade angle at exit, deg	55	35	50	40	40
Exit blade height, in.	5.4096	0.203	0.656	0.413	0.653
Ratio of exit axial clearance to exit blade height	0.042	0.050	0.0253	0.023	0.023
Diffuser:					
Type	Wedge	Cambered vane	Wedge	Cambered vane	Cambered vane
Number of vanes	23	27	24	21-21	21-21
Inlet flow angle, deg	70	73	75.1	73	73
Area ratio	2.9	2.5	2.75	~1.6	~1.6
Channel divergence	7.65	7	7.8	~6	~6
Inlet Reynolds number, V_2b_2/ν_2	10^6	0.3×10^6	0.6×10^6	1.6×10^6	2.5×10^6

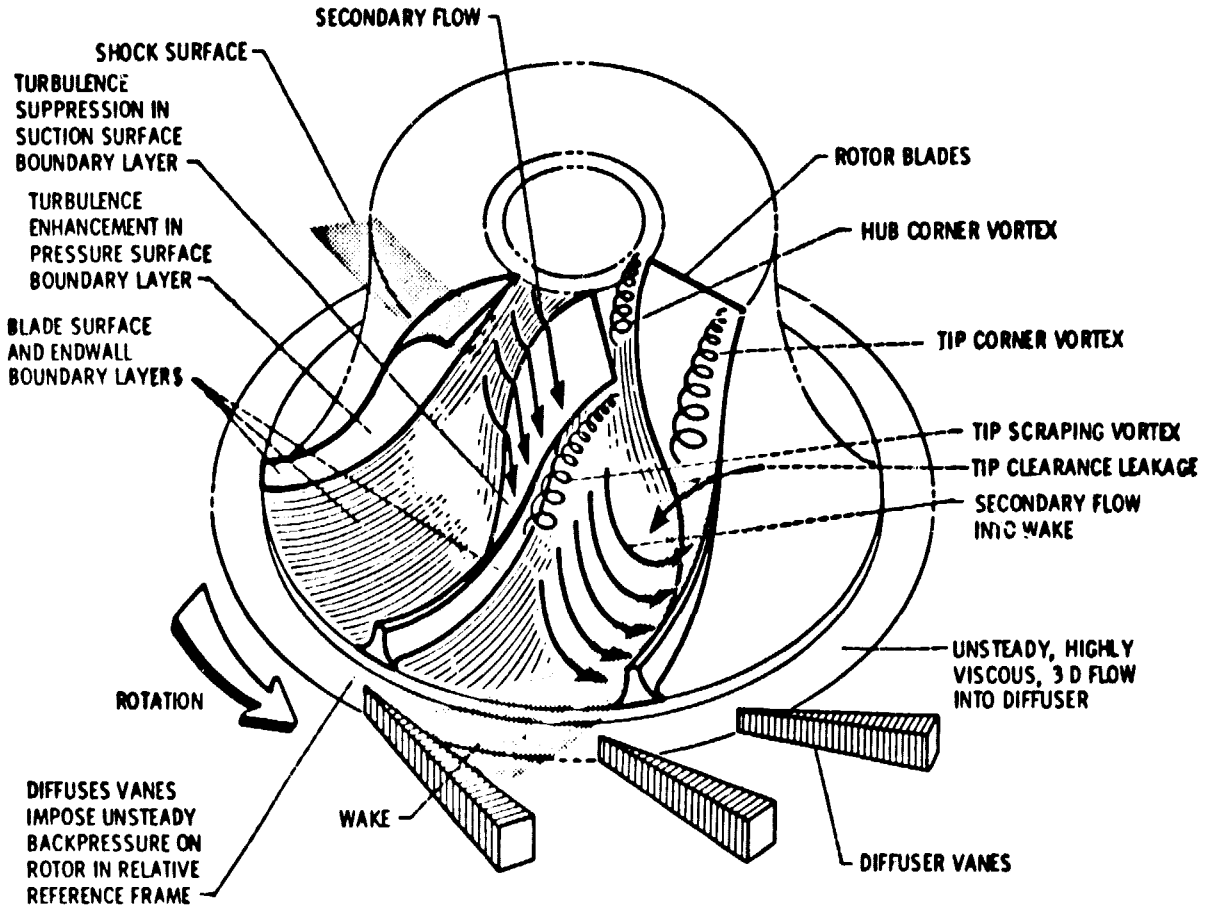

Figure 1. - Centrifugal compressor flow phenomena.

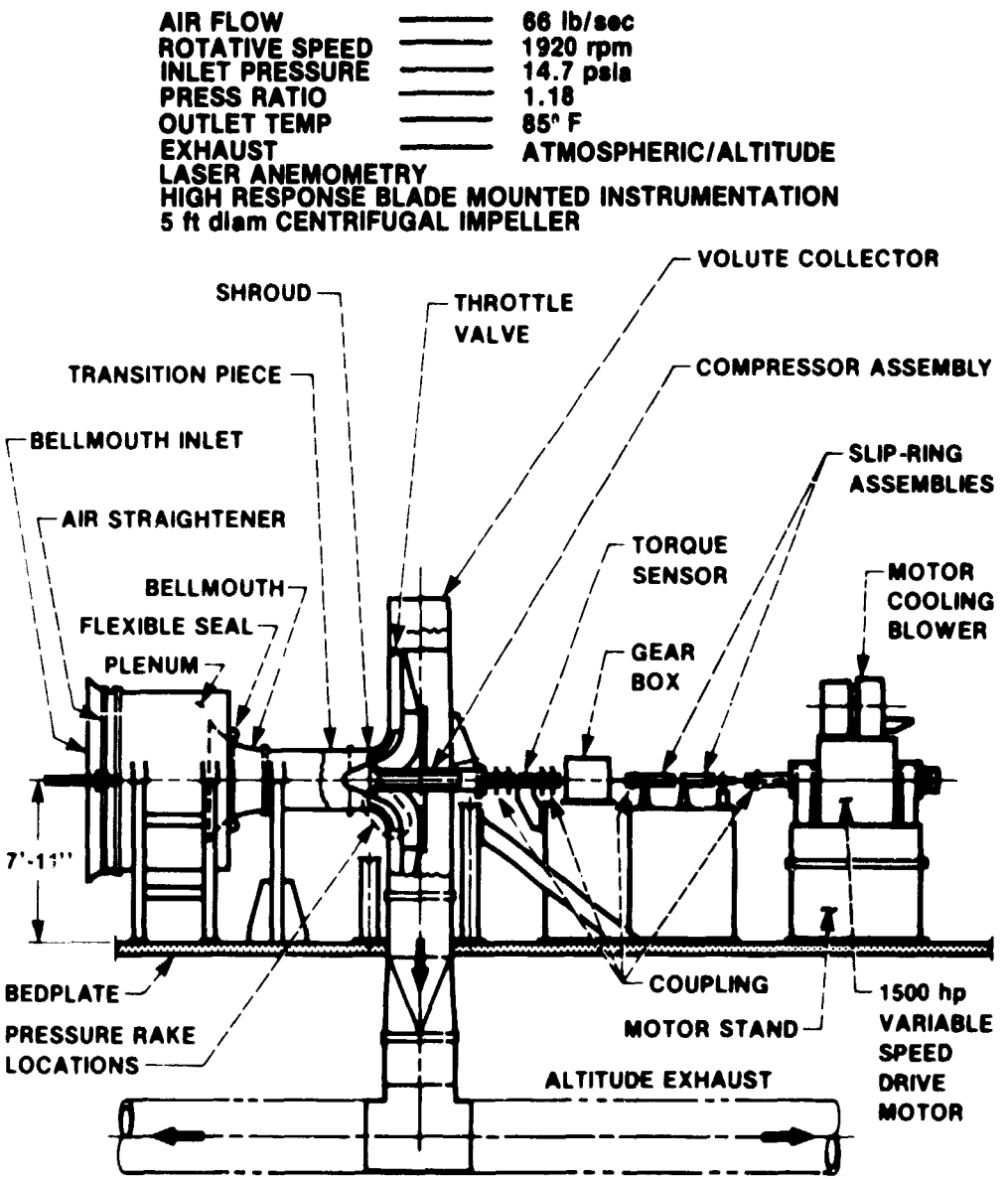

Figure 2. - Low-speed centrifugal compressor facility.

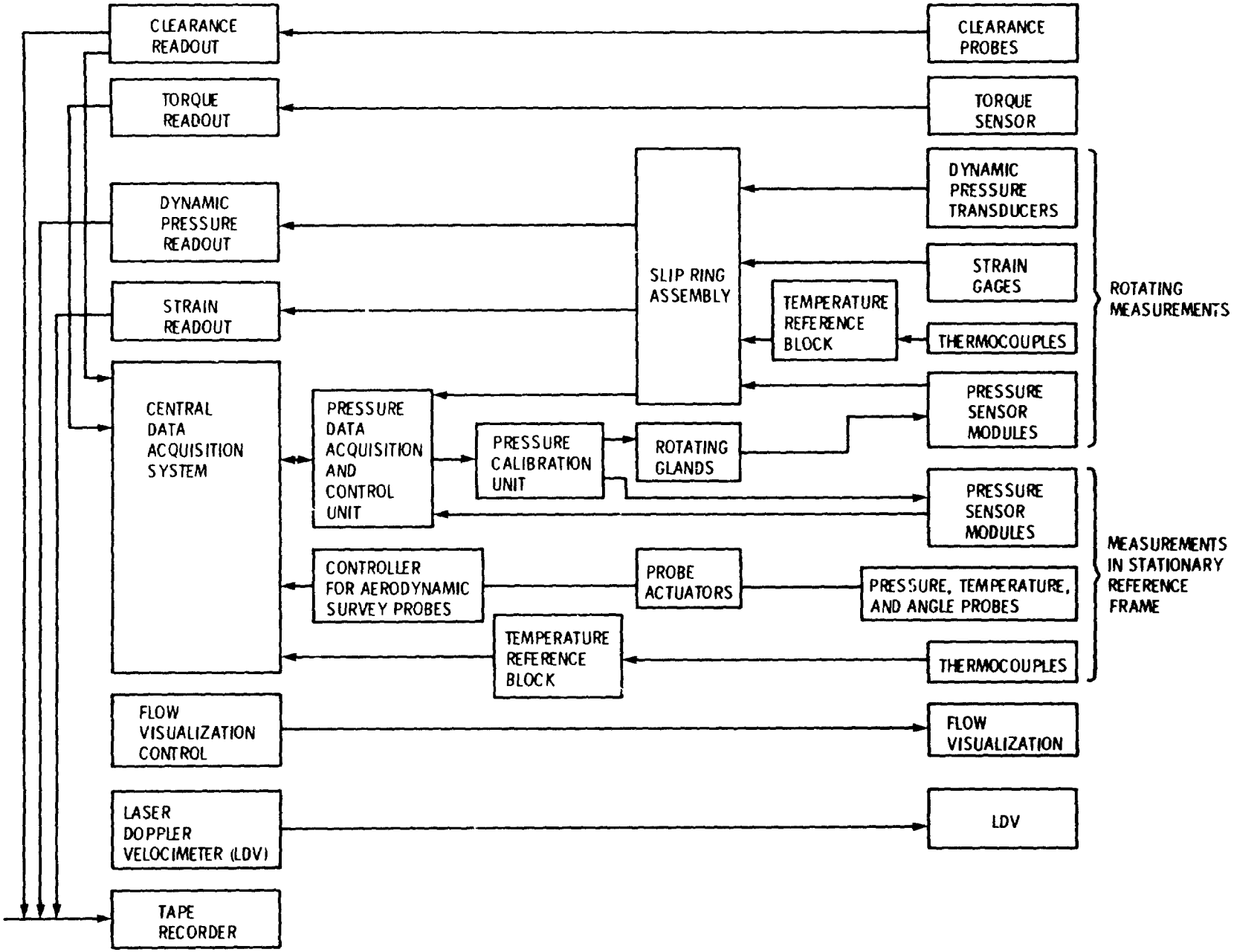

Figure 3. - Block diagram of instrumentation system.

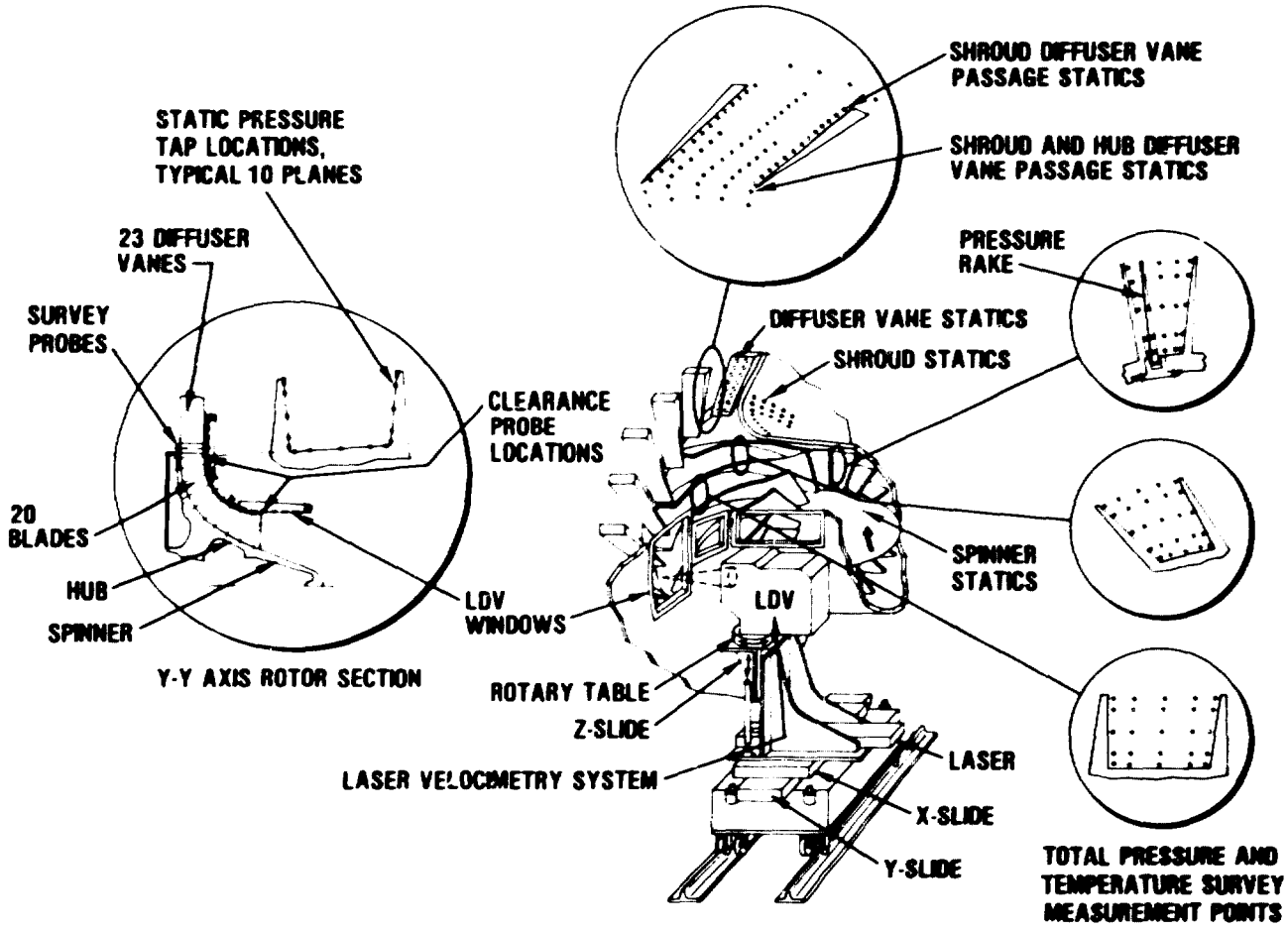

Figure 4. - Low-speed centrifugal compressor instrumentation.

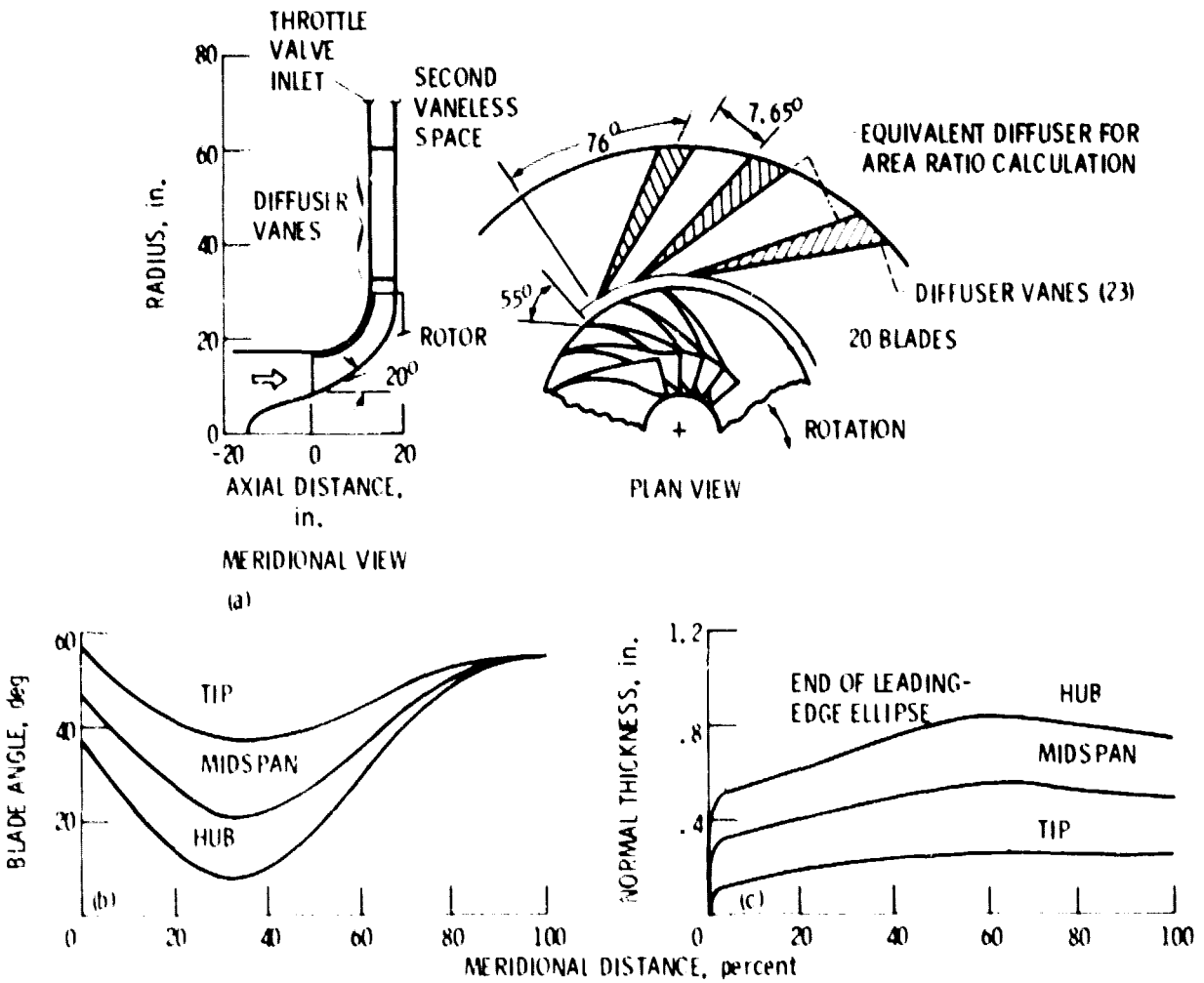

(a) Meridional and plan view.
(b) Blade mean camber line distribution for hub, midspan, and tip.
(c) Blade normal thickness distribution for hub, midspan, and tip.

Figure 5. - Configuration of low-speed centrifugal compressor initial stage.

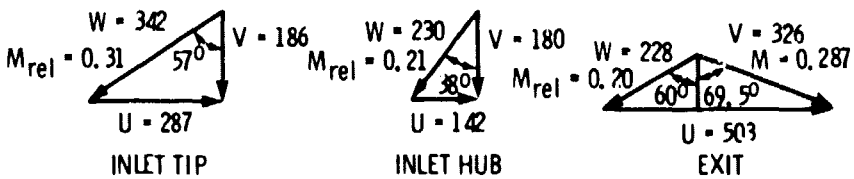

(a)

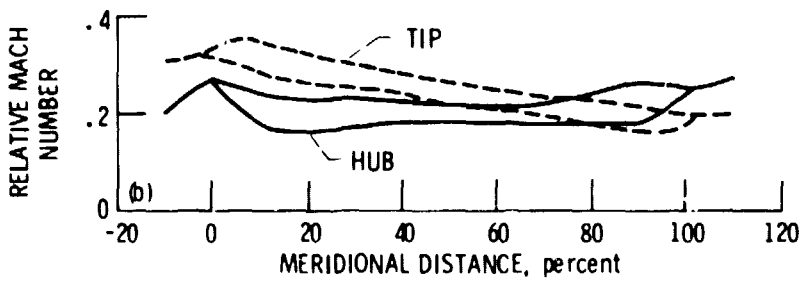

(a) Rotor vector diagrams from preliminary design code. (Velocities in feet per second.)

(b) Blade surface Mach numbers obtained with three-dimensional Euler code.

Figure 6. - Aerodynamic design of low-speed centrifugal compressor initial stage.